

# Dynamic Theory of Intermodulation Distortion

THOMAS C. BEST, MEMBER, IEEE, CHARLES A. LEE, MEMBER, IEEE, AND G. CONRAD DALMAN, FELLOW, IEEE

**Abstract** — This paper studies the third-order intermodulation distortion of signals in a reflection amplifier that are separated by an appreciable fraction of the bandwidth. This large separation of input signals requires taking account of the energy interchange between diode and circuit. A theory of intermodulation distortion accounting for this interaction is developed for large-order nonlinearities. Previous analyses of this problem have been limited to small nonlinearities and small separation of the input signals. Experimental verification of the theory developed here is demonstrated for an IMPATT diode reflection amplifier as a function of power level and tone separation.

## I. INTRODUCTION

IN ORDER TO BE able to design high-quality high-power wide-bandwidth satellite communication systems, a theoretical understanding of the intermodulation distortion produced by signals arbitrarily placed within the band must be developed. This arbitrary separation of input signals requires accounting for the energy interchange between device and circuit. This paper presents a theory for such interaction in the presence of large-order nonlinearities.

Intermodulation distortion is usually measured with two very closely spaced signals as a function of the input power. In this situation the envelope frequency of the two input signals is much less than the amplifier bandwidth. For this case the diode amplitude follows the input signal amplitude and a theoretical description has been given by H. Komizo *et al.* [1]. For tone separations comparable to or greater than the amplifier bandwidth, the energy exchange between diode and circuit must be taken into account. Javed *et al.* [2] have included device-circuit energy interchange in their analysis, but their series solution is limited to very small nonlinearities and they have examined experimentally only very small tone separations.

The significant difference of the theory developed here is that the nonlinear amplifier response to the amplitude of the combined input signals is solved in the time domain. Two coupled first-order differential equations in amplitude and phase of the envelope are derived using the slowly

Manuscript received August 25, 1981; revised December 21, 1981. This work was supported in part by the Air Force Avionics Laboratory, Air Force Systems Command, USAF, Wright-Patterson Air Force Base, OH 45433, under Contract F33615-80-C-1045.

T.C. Best was with Cornell University, Ithica, NY. He is now with TRW Electronics Systems Group, Redondo Beach, CA 90278.

C.A. Lee and G.C. Dalman are with Cornell University, School of Electrical Engineering, Phillips Hall, Ithica, NY 14853

varying amplitude approximation. These differential equations are solved numerically and thus large nonlinearities present no special problem in calculating the distortion. This theory is applicable to both three- and two-terminal amplifier circuits but this paper deals only with a single-tuned reflection amplifier for simplicity. In addition, for the first time experimental data for large tone separations are presented and analyzed.

## II. EXPERIMENT

Fig. 1 shows a block diagram of the experimental setup. A narrow-band single-resonance high-gain amplifier was the subject of the experimentation. There were two main reasons for its choice. The first was that relatively large voltages would be developed across the diode chip for medium input powers, thus allowing a large diode nonlinearity to be explored without the need for a high-power TWT amplifier. The second reason was that smaller frequency differences would be required to develop a significant phase shift between the input and output signals. A final factor in the circuit choice was its simplicity, which allows for a much easier theoretical representation and understanding. The first step of the analysis was to characterize the diode circuit, and the diode itself. This was done by generating a power-in versus power-out curve, as is shown in Fig. 2. Curves of reflected power versus frequency were recorded for various input power levels, and two such cases are shown in Figs. 3 and 4. The normalized negative conductance  $g$  can now be found since

$$\text{Gain} = \frac{P_{\text{out}}}{P_{\text{in}}} = \left(1 - \frac{Q_x}{Q_a}\right)^2 / \left(1 + \frac{Q_x}{Q_a}\right)^2 \quad (1)$$

$$g = \frac{Q_x}{Q_a} = \left[1 - (P_{\text{out}}/P_{\text{in}})^{1/2}\right] / \left[1 + (P_{\text{out}}/P_{\text{in}})^{1/2}\right] \quad (2)$$

where  $Q_x$  and  $Q_a$  are the external and amplifier quality factors. This information is used to create a graph of the negative conductance versus the square root of the normalized input power  $(P_{\text{in}}/P_{\text{in},\text{max}})^{1/2}$  and is shown in Fig. 5.

The external  $Q_x$  was found by determining the small signal negative conductance  $g_{ss}$  from (2) and determining the loaded  $Q_L$  which is also related to  $Q_x$  by the following expression:

$$\frac{1}{Q_x} + \frac{1}{Q_a} = \frac{1}{Q_L} = \frac{\Delta f_{1/2}}{f_0} \quad (3)$$

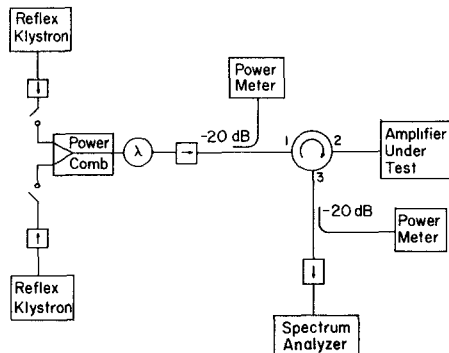


Fig. 1. Block diagram of microwave test setup for measuring reflection amplifier intermodulation distortion.

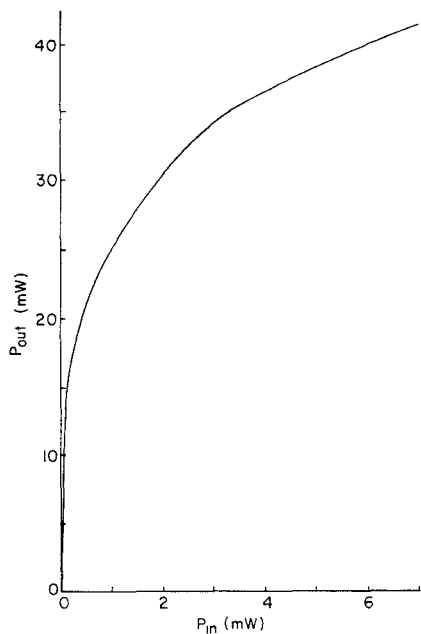


Fig. 2. Power-out versus power-in for the amplifier used in the distortion measurements.

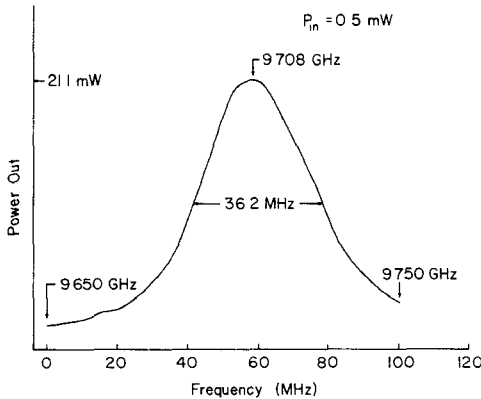


Fig. 3. Power-out versus frequency of the amplifier for an input power level of 0.5 mW.

where  $\Delta f_{1/2}$  is the half-power bandwidth, and  $f_0$  is the center frequency. The amplifier circuit used for the intermodulation distortion measurements was thus determined to have a  $Q_x$  of 60.

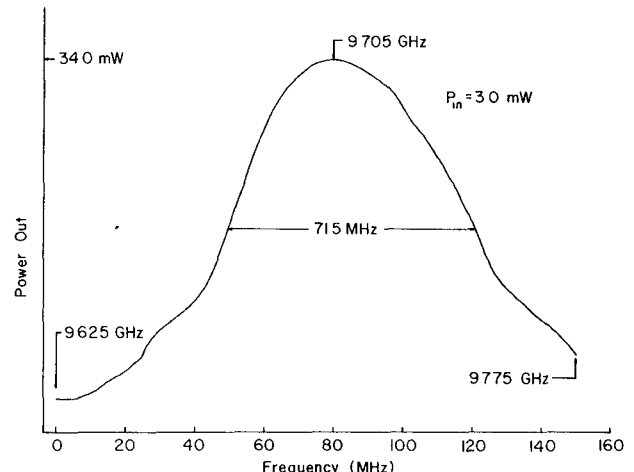


Fig. 4. Power-out versus frequency of the amplifier for an input power level 3.0 mW.

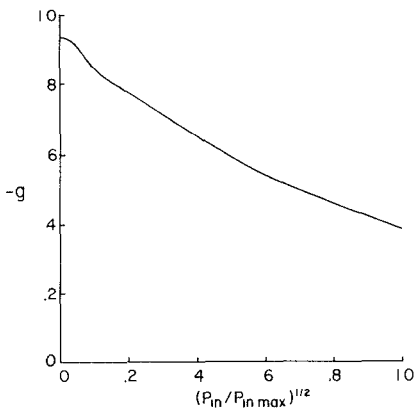


Fig. 5. Normalized diode negative conductance as a function of the normalized voltage amplitude of the incident signal [ $(P_{in})_{max} = 8.0$  mW].

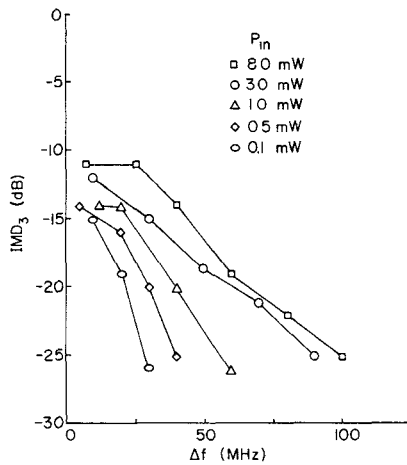


Fig. 6. Measurements of third-order intermodulation distortion versus tone separation at various input power signal levels.

Finally, measurements of the level of third-order IMD versus  $\Delta f$ , the separation of the two tones, were made on a spectrum analyzer for various input power levels. These results are shown in Fig. 6. The curves shown in Fig. 6 are the average of the upper and lower intermodulation sidebands.

### III. THEORY

Let us first consider a model for the IMPATT diode amplifier which is shown schematically in Fig. 7. In the figure, the  $ABCD$  matrix represents a lossless network which defines the amplifier gain and bandwidth, planes (1) and (2) are the reference planes of the diode circuit and diode chip, respectively,  $Y_D$  is the diode chip admittance,  $Y_0$  is the characteristic line admittance,  $Y_1$  is in amplifier input admittance, and  $Y_L$  is the circuit load admittance presented to the diode.  $P_{in}$  and  $P_{out}$  are the input and output powers and  $V_{rf}$  is the peak ac voltage across the diode chip.

The reflection coefficient at plane (1) is given by the relationship

$$\begin{aligned}\rho_1 &= (Y_0 - Y_1)/(Y_0 + Y_1) \\ &= [(Y_L^* - Y_D)/(Y_L + Y_D)] \exp(-j\beta)\end{aligned}\quad (4)$$

where

$$\exp(-j\beta) = (-Y_0 B + D)/(Y_0 B + D). \quad (5)$$

The assumption of a lossless network means that the element  $B$  is pure imaginary and the element  $D$  is real, thus making the phase angle  $\beta$  real.

The amplifier distortion we wish to calculate arises from the nonlinear diode response to the input signal. One must first set down the relation between the incident input signal and the diode voltage which is the sum of the incident and reflected waves

$$V_{rf} = V_{2+} + V_{2-} = V_{2+}(1 + \rho_2) \quad (6)$$

where  $V_{2+}$  and  $V_{2-}$  are the incident and reflected waves at plane (2) and  $\rho_2$  is the reflection coefficient at that plane. This reflection coefficient is given by

$$\rho_2 = \frac{Y_L^* - Y_D}{Y_L + Y_D} \quad (7)$$

and differs from  $\rho_1$  defined in (4) by only the phase factor of (5). From (6) one obtains the relation

$$V_{2+} = \frac{1}{2}(1 + g + jb)V_{rf} \quad (8)$$

where

$$g \equiv G_D/G_L, \quad b \equiv (B_L + B_D)/G_L.$$

This relation can be interpreted in a normal way if the voltages are single harmonic components with  $g$  and  $b$  being the normalized conductance and susceptance at the frequency of interest. For the measurement of intermodulation distortion, however, the signal  $V_{2+}$  has the form

$$V_{2+} = 2V_0 \cos pt \cos \omega_0 t \quad (9)$$

where

$$p = 1/2(\omega_2 - \omega_1) \quad \omega_0 = 1/2(\omega_1 + \omega_2).$$

In addition, the diode nonlinearity produces harmonic components in  $V_{rf}$ . To handle this situation we can regard  $g$  and  $b$  as differential-integral operators in the time domain. Then by using the slowly-varying amplitude ap-

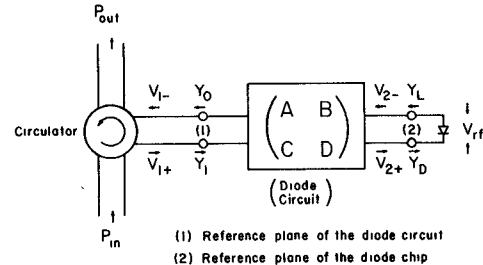


Fig. 7. Schematic representation of the reflection amplifier showing reference planes and admittances at those planes.

proximation one can derive a differential equation in time which describes the diode-circuit behavior at low frequencies but contains admittance components evaluated at  $\omega_0$ .

For this singly-tuned resonant cavity used in the experiment, (8) takes the form

$$\begin{aligned}V_{2+} &= \frac{1}{2} \left\{ 1 + g_{ss} + \frac{\Delta \hat{Y}_D}{G_L} \right. \\ &\quad \left. + \frac{C + C_0}{G_L} \frac{d}{dt} + \frac{1}{G_L} \left( \frac{1}{L} + \frac{1}{L_{ss}} \right) \int dt \right\} V_{rf} \quad (10)\end{aligned}$$

where  $g_{ss}$  is the normalized small signal diode conductance,  $C$  and  $L$  are the equivalent cavity capacitance and inductance, and  $C_0$  and  $L_{ss}$  denote the diode transition capacitance and electronic inductance, respectively. The operator  $\Delta \hat{Y}_D$  represents the deviation of the diode admittance from the small signal values indicated in (10).

To reduce (10) to a differential equation on the slowly-varying part of  $V_{rf} = A(t) e^{j\omega_0 t}$  we use the relations

$$e^{-j\omega_0 t} \frac{d}{dt} V_{rf} = \frac{dA}{dt} + j\omega_0 A \quad (11)$$

and

$$e^{-j\omega_0 t} \int dt V_{rf} = \frac{1}{j\omega_0} A + \frac{1}{\omega_0^2} \frac{dA}{dt}. \quad (12)$$

Equations (11) and (12) are readily obtained by operating on the Fourier transform of  $V_{rf}$ . Substituting these back into (10) one obtains

$$4V_0 \cos pt = 2\mathcal{C} \frac{dA}{dt} + (1 + g_{ss})A + e^{-j\omega_0 t} \Delta \hat{Y}_D V_{rf} \quad (13)$$

where

$$\mathcal{C} = (C + C_0)/G_L \quad \mathcal{L}^{-1} = (L^{-1} + L_{ss}^{-1})/G_L$$

$$\omega_0^2 = 1/\mathcal{C}\mathcal{L} \quad \Delta \hat{Y}_D = \Delta \hat{Y}_D/G_L.$$

The remaining task is to evaluate the final term in (13). Using the Fourier transform of  $V_{rf}$  again and expanding the admittance function about  $\omega_0$  and the amplitude of the ac voltage across the diode  $V_1$ , one obtains

$$\begin{aligned}e^{-j\omega_0 t} \Delta \hat{Y}_D V_{rf} &= \frac{dA}{dt} \left( -j \frac{\partial g}{\partial \omega_0} + \frac{\partial b}{\partial \omega_0} \right) \\ &\quad + A \sum_{k=1}^{\infty} \frac{\partial^k Y_D}{\partial V_1^k} \frac{V_1^k}{k!} \quad (14)\end{aligned}$$

where only the first order term in the Taylor expansion is necessary with respect to  $\omega_0$  but all the higher order terms in the expansion with respect to  $V_1$  are included because we are interested in being able to handle large nonlinearities. Inserting (14) back into (13) we obtain

$$4V_0 \cos pt = \frac{dA}{dt} \left[ 2\mathcal{C} - j \frac{\partial g}{\partial \omega_0} + \frac{\partial b}{\partial \omega_0} \right] + [1 + g + jb] A \quad (15)$$

where

$$1 + g_{ss} + \sum_{k=1}^{\infty} \frac{\partial^k y_D}{\partial V_1^k} \frac{V_1^k}{k!} = 1 + g + jb.$$

The slowly-varying coefficient  $A$  contains both the amplitude and phase of the diode voltage amplitude  $A(t) = V_1 e^{j\phi}$ . Putting this relation into (15) and separating the real and imaginary components gives

$$4V_0 \cos pt \cos(\phi + \gamma) = 2\mathcal{C}_{eq} \frac{dV_1}{dt} + \sqrt{(1+g)^2 + b^2} \cos(\Theta - \gamma) V_1 \quad (16a)$$

$$-4V_0 \cos pt \sin(\phi + \gamma) = 2\mathcal{C}_{eq} \frac{d\phi}{dt} V_1 + \sqrt{(1+g)^2 + b^2} \sin(\Theta - \gamma) V_1 \quad (16b)$$

where we have used

$$2\mathcal{C} - j \frac{\partial g}{\partial \omega_0} + \frac{\partial b}{\partial \omega_0} = 2\mathcal{C}_{eq} e^{j\gamma}$$

and

$$\tan \theta = \frac{b}{1+g}.$$

Equations (16a) and (16b) may be further simplified by considering a case where  $b = 0$ , giving  $\theta = 0$  and letting  $\gamma = 0$ , to obtain

$$\cos(2\pi y) \cos \phi = \frac{K}{2\pi} \frac{du}{dy} + (1+g)u \quad (17a)$$

$$-\cos(2\pi y) \sin \phi = \frac{K}{2\pi} \frac{d\phi}{dy} u \quad (17b)$$

where

$$2\pi y = pt \quad K = 2Q_x p / \omega_0 \quad u = V_1 / 4V_0 \quad Q_x = \omega_0 \mathcal{C}_{eq}$$

Upon examining (17b) one notes that when  $u = 0$  then  $\phi$  must also be zero to avoid a singularity in  $d\phi/dy$ . When both (17a) and (17b) are solved simultaneously one obtains  $\phi = 0$  as a solution, leaving just one equation to be solved, namely

$$\frac{du}{dy} = \frac{2\pi}{K} [\cos(2\pi y) - (1+g)u]. \quad (18)$$

Equation (18) has been used to calculate the intermodulation distortion for the experimental measurements made on an IMPATT diode amplifier.

The outline of the expected response of the diode voltage to varying separation of the two tones can be seen from

solving (18) for the case where the diode conductance  $g$  is independent of  $V_1$ . An analytic solution can be obtained for this case in the form

$$u(y) = \frac{1}{[(1+g)^2 + K^2]^{1/2}} \cos(2\pi y - \psi) \quad (19)$$

where

$$\tan \psi = K/(1+g).$$

One can see from this expression that  $u$  responds in phase to the incident signal for very small  $K$  (i.e., small separation of the two tones), and lags by  $90^\circ$  when the tone separation is much greater than the bandwidth of the amplifier.

#### IV. RESULTS

In order to compare the results of the theory with those of the experiment, it is first necessary to fit the diode conductance found experimentally to a polynomial in  $u$  so it can be included in (18). This relation  $g(u)$  is found from the experimental data by first choosing  $(P_{in})_{max}$ . The input power scale is then normalized to this  $(P_{in})_{max}$ , giving

$$\cos pt = [P_{in}/(P_{in})_{max}]^{1/2}. \quad (22)$$

Using the value of  $g$  calculated from (2), the normalized diode voltage  $u$  is calculated from the expression

$$u = \cos pt / (1+g). \quad (23)$$

A least-squares routine was used to fit the curve of  $g$  to a fifth-order polynomial in  $u$ . This was done for two different cases,  $P_{in} = 0.5$  mW and  $P_{in} = 3$  mW, and the results are shown in Figs. 8 and 9, respectively.

Equation (18) can now be solved by a fourth-order Runga-Kutta routine. Initial results were obtained on an HP-97 calculator, but for the final results a PDP-11 was used because of its increased speed. Fig. 10 shows several solutions to (18) of the diode voltage versus time. The increasing phase shift of the diode voltage can be seen as  $K$  increases, corresponding to a larger tone separation. The distortion present in Fig. 10 can be seen more clearly by plotting  $u$  versus  $\cos pt$  as shown in Fig. 11. The smallest value of  $K = 0.05$  corresponds to a tone separation of 6 MHz which is less than 10 percent of the half-power bandwidth, but as is evident in Fig. 11 there is still a pronounced effect due to energy interchange between the diode and the cavity.

The intermodulation distortion is given by the ratio of the third-harmonic component of  $u \rightarrow u(3)$  to the first-harmonic component of the reflected wave  $u^{(1)}$ . The fundamental component of the diode voltage is given by

$$u^{(1)} = \sqrt{a_1^2 + b_1^2} \quad (24)$$

where

$$a_1 = 2 \int_0^1 u \cos(2\pi y) dy$$

and

$$b_1 = 2 \int_0^1 u \sin(2\pi y) dy.$$

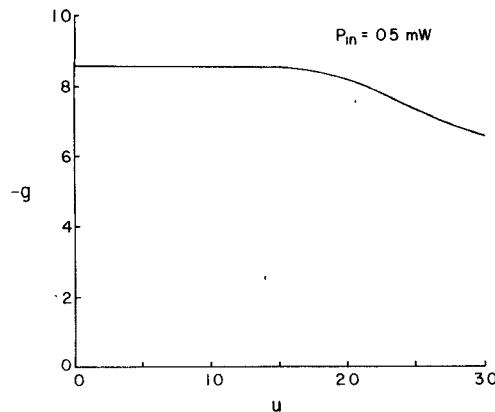


Fig. 8. Normalized diode negative conductance as a function of the normalized chip voltage for an input power level of 0.5 mW.

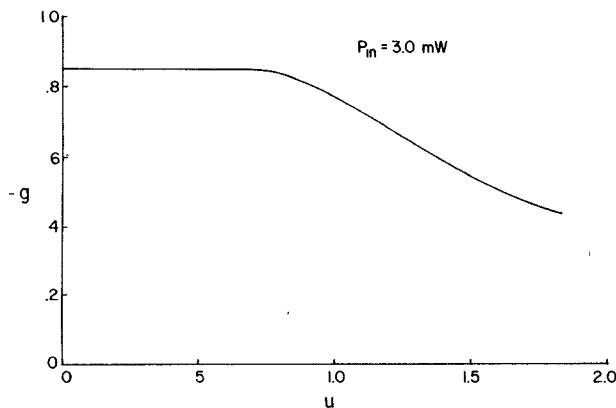


Fig. 9. Normalized diode negative conductance as a function of the normalized chip voltage for an input power level of 3.0 mW.

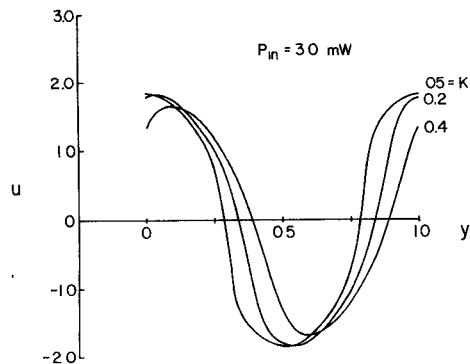


Fig. 10. Calculated normalized diode voltage versus time for several different separations of the two tone input signal.

Similarly, for the third harmonic

$$u^{(3)} = \sqrt{a_3^2 + b_3^2} \quad (25)$$

where

$$a_3 = 2 \int_0^1 u \cos(6\pi y) dy$$

and

$$b_3 = 2 \int_0^1 u \sin(6\pi y) dy.$$

To calculate the amplitude of the reflected fundamental

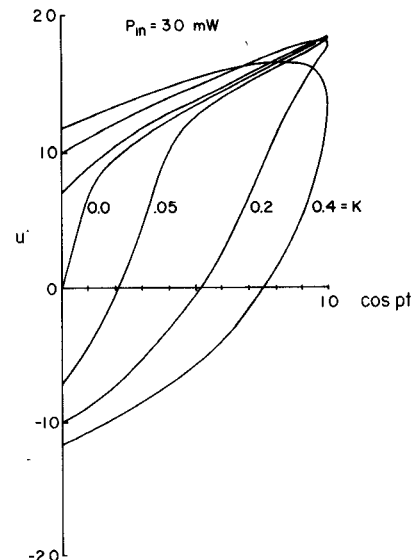


Fig. 11. Calculated normalized diode voltage versus the amplitude of the input signal envelope for several tone separations.

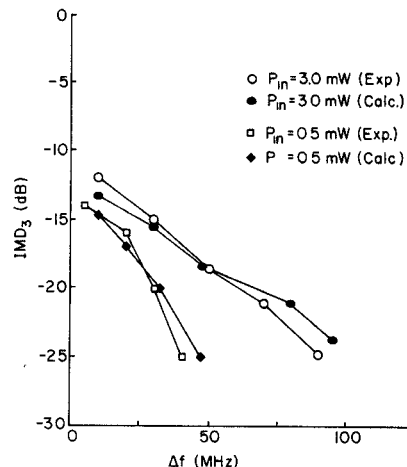


Fig. 12. Comparison of measured and calculated intermodulation distortion as a function of tone frequency separation for average input power levels of 0.5 and 3.0 mW.

component one subtracts the amplitude of the incident signal

$$u_-^{(1)} = u^{(1)} - 0.5 \quad (26)$$

where

$$u_+^{(1)} = (\cos pt)/2.$$

Since there is no incident signal at the third harmonic  $u^{(3)} = u_-^{(3)}$ . Finally, the third-order intermodulation distortion in decibels is given by

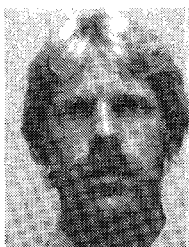
$$\text{IMD} = 20 \log_{10} |u_-^{(3)} / u_-^{(1)}|. \quad (27)$$

The distortion of the amplifier at two different power levels, 0.5 and 3.0 mW, was compared to theory as a function of the tone separation using the experimentally determined value  $Q_x = 60$  and the results are shown in Fig. 12. The agreement is quite good for the simple case considered. The theory presented here should be applicable to broadband circuits and to three-terminal amplifiers as well.

## REFERENCES

- [1] H. Komizo, Y. Daido, H. Ashida, Y. Ito, and M. Honma, "Improvement of nonlinear distortion in an IMPATT stable amplifier," *IEEE Trans. Microwave Theory Tech.*, MTT-21, pp. 721-728, Nov. 1973.
- [2] A. Javed, B. Syrett, and P. Goud, "IMD analysis of reflection type IMPATT amplifiers using Volterra series representation," *IEEE Trans. Microwave Theory Tech.*, MTT-25, pp. 729-734, Sept. 1977.

+



Thomas C. Best

Thomas C. Best (S'78-M'81) was born in Amsterdam, N.Y., on May 24, 1958. He received the B.S. and M.E.E. degrees in electrical engineering from Cornell University, Ithaca, N.Y., in 1980 and 1981, respectively.

In 1981 he joined the Millimeter Wave Technology Department of TRW as a member of the technical staff. He is presently involved in the design and development of wideband millimeter-wave IMPATT amplifier circuits and the implementation of an automated network analyzer.

+



Charles A. Lee (M'69) was born in New York, NY, on August 28, 1922. He received the B.E.E. degree in communications from Rensselaer Polytechnic Institute, Troy, NY, in 1944, and a Ph.D. in physics from Columbia University, New York, NY, in 1953.

After a year of postdoctoral work at Columbia University working on molecular beam analysis of nuclear hyperfine structure of excited states of Rubidium, he joined Bell Telephone Laboratories, Murray Hill, as a member of the technical staff in 1953. At Bell Laboratories he started research in the physics of new devices and device concepts. With W. Shockley he invented and successfully realized the diffused base transistor which, at that time, raised the upper frequency limit of transistors an order of magnitude to 0.7 GHz. Subsequent work included the temperature variation of noise in transistors and diodes, the first reported p-n junctions in InSb, internal field emission in narrow silicon and germanium junctions, and the mea-

surement of electron-hole ionization coefficients in silicon. This last work on avalanche phenomena led to the fabrication and analysis of the first Read diode, a microwave negative resistance device.

He joined the Faculty of the School of Electrical Engineering at Cornell University in the Fall of 1967. With his students he has developed the large signal Quasi-Static theory of avalanche devices, and made the first high efficiency silicon Schottky barrier avalanche diodes. His recent research concerns ion-implanted Read diodes in various semiconductors, ionization coefficient measurements, and the analysis of submicron avalanche regions.

Professor Lee is a member of the American Physical Society, Sigma Xi, Tau Beta Pi, Eta Kappa Nu, and the American Association for the Advancement of Science.

+



G. Conrad Dalman

G. Conrad Dalman, (S'40-A'41-SM'51-F'65) born in Winnipeg, Canada, received the B.E.E. degree from the City College of New York and the M.E.E. and D.E.E. degrees from the Polytechnic Institute of Brooklyn. He was associated with RCA (1940-45), Bell Telephone Laboratories (1945-47), and the Sperry Gyroscope Co. (1949-56), primarily in the vacuum-tube and microwave fields. While in industry he served as an Adjunct Professor at the Polytechnic Institute of Brooklyn and as a Lecturer at the City College of

New York.

In 1956 he joined Cornell University as Professor of Electrical Engineering and initiated graduate research programs in microwaves. At present he is active in high power IMPATT diode and millimeter-FET research and in undergraduate and graduate teaching. He has served as a consultant to several industrial firms and currently is a consultant to TRW, Redondo Beach, CA. He spent his 1980-81 sabbatical year with TRW working with their millimeter-wave IMPATT amplifier group. During his 1962-63 sabbatical year he served as Project Manager, China Project, for the United Nations at Chiao Tung University, Hsin Chu, Taiwan. From 1975 to 1980 he served as Director of the School of Electrical Engineering and as Acting Director from 1972 to 1973.

Dr. Dalman is a member of Sigma Xi, Eta Kappa Nu, Tau Beta Pi, and the American Associate for the Advancement of Science. He is a Fellow member of the AAAS, and he received an IEEE Fellow Award for his industrial work on microwave oscillators and amplifiers. He also received a Certificate of Distinction from the Polytechnic Institute of Brooklyn.